CLAY MINERAL REACTION-PROGRESS – THE MATURITY AND BURIAL HISTORY OF THE LIAS GROUP OF ENGLAND AND WALES

S. J. KEMP, R. J. MERRIMAN and J. E. BOUCH

British Geological Survey, Sir Kingsley Dunham Centre,

Keyworth, Nottingham, UK. NG12 5GG

sjk@bgs.ac.uk

ABSTRACT

The clay mineral assemblages and microtextures of a suite of mudrocks from the Lias Group of England and Wales indicate important regional differences in burial history.

Samples from the northern Cleveland Basin are characterised by illite/smectite (I/S, 90% illite) and little carbonate whilst samples from the southern Worcester and Wessex basins contain less mature discrete smectite and are often calcite- and dolomite-rich. Lias Group rocks have been buried to 4-km in the Cleveland Basin but to less than 2-km in the Worcester and Wessex basins. Burial in the Cleveland Basin is deeper than previously estimated and does not need a local heating event. Illite/smectite (80% illite) detected in samples from the East Midlands Shelf suggests burial to 3-km, again deeper than previous estimates for this region.

KEYWORDS: Clay diagenesis, Lias Group, illite/smectite, smectite, XRD, SEM, TEM, surface-area, basin maturity

Clay mineral reaction-progress – The maturity and burial history of the Lias Group of England and Wales

Introduction

Because of its relatively good coastal and quarry exposure, the onshore English Lias Group has attracted a number of mineralogical studies, including clay mineralogy. Several brief studies were carried out in the 1960s on outcrops in southern England (e.g. Hallam, 1960; Cosgrove & Salter, 1966). Later, Pye & Krinsley (1986) examined Lias Group rocks from the Cleveland Basin using the then recent development of backscattered scanning electron microscopy and were followed by van Buchem *et al.* (1992).

As part of a site-investigation for a low-level radioactive waste repository at Fulbeck, Lincolnshire, Bloodworth *et al*. (1987) carried out an extensive mineralogical and lithogeochemical study of borehole material from the Lower and Middle Lias sequence of interbedded mudstones and limestones. Another borehole sequence of Lias mudstones from the Copperhill Quarry, near Ancaster, Lincolnshire, was studied by Mitchell (1992) in order to identify any potential clay 'marker' horizons or distinctive variations in clay mineral assemblages. Kemp & Hards (2000) also investigated the mineral assemblages of Lias samples from two site-investigation boreholes sited near the M5 motorway in Gloucestershire. Most recently, Deconinck *et al.* (2003) presented a dataset including clay mineral assemblages, gamma-ray spectrometry, organic-matter content and magnetic susceptibility for the Blue Lias Formation in Dorset and Somerset. However, despite this intensive and continuing interest in the Lias, no regional interpretation of the clay mineral assemblages has been attempted to date.

Sedimentary basins, such as those represented by the Lias Group, are crustal depressions where clay minerals formed, by surface weathering and pedogenic processes are ponded, in some cases forming up to 65-70% of basinal sediments (Potter *et al.*, 1980). Because of their thermodynamic metastability, clay minerals are particularly sensitive to changes in the shallow crustal conditions that control the thermal history of sedimentary basins. Following from the seminal work of Hower *et al.* (1976), clay mineral transformations (reactions) resulting from burial in sedimentary basins have been widely studied and increasingly used to model basin thermal history. During sedimentary burial, a progressive series of clay mineral reactions convert soft mud to hard lithified mudstone and shale. Quantitatively, the most important series of reactions responsible for the lithification of mud is the progressive transformation of smectite to illite via a series of intermediate illite/smectite (I/S) mixed-layer minerals. Progress of this series of dehydration reactions increases the density of the mudstone by mobilising fluids, and also reducing pore-space as a new, bedding-parallel illite invades and fills voids (Merriman & Peacor, 1999). The progress of the smectite–to–illite reaction can be measured using X-ray diffraction (XRD)-based techniques such as computer modelling of the percentage illite in I/S, and measuring changes in 'illite crystallinity' using the Kubler index (KI). Changes in KI caused by diagenetic burial and very low-grade metamorphism have been correlated with transmission electron microscopy (TEM) measurements of illite crystallite thickness from a variety of mudrocks including mudstone, shale and slate samples (e.g. Warr & Nieto, 1998; Merriman & Peacor, 1999, fig. 2.19). These show that during burial diagenesis, illite crystallites progressively increase in mean thickness from 2 or 3 (10-Å) layers to 20-25 (10-Å) layers, prior to the onset of very low-grade metamorphism. Progressive increases in illite crystallite thickness are not reversed by basin inversion and uplift and can be used to estimate maximum burial depth, particularly when used with other indicators of thermal maturity such as vitrinite reflectance or apatite fission track analysis. Reaction-progress in clay minerals in relation to changes observed in organic materials have been used to construct a Basin Maturity Chart summarizing these depth-dependant changes (Merriman & Kemp, 1996; Merriman & Frey, 1999).

This study uses regional variations in clay mineral assemblages and reaction-progress to explore the thermal maturity and burial history of the onshore Lias Group in the UK.

GEOLOGICAL SETTING

The Lower Jurassic (Lias, or in strict lithostratigraphical terminology the Lias *Group*) of England and Wales forms a thin, approximately continuous northeast-southwest trending outcrop, extending southwards from Redcar on the Cleveland coast, through Lincolnshire, the Midlands, the Cotswolds and Somerset, to Lyme Regis on the Dorset coast. Isolated outcrops of the Lias also occur in west Somerset, south Wales and Cheshire (Figure 1). In general, the strata dip very gently towards the east or south-east beneath younger beds, so that the Lias is present at depth to the east of the main outcrop, other than in the London area (Cox *et al.*, 1999). It comprises shallow marine intercalated mudstones, shales and muddy limestones deposited in an extensive epicontinental (or epeiric) sea during the major world-wide transgression that marked the end of the Triassic (Anderton *et al.* 1979). Thick mudstone sequences were deposited in a series of basins whereas thin calcareous and sandy deposits were formed in shallow shoals. Three structural highs in the Mendips, Moreton-in-the-Marsh and Market Weighton separated areas of substantial subsidence and controlled sedimentation throughout the Jurassic. As a result the Lias is characterised by considerable lateral variations in thickness.

In an attempt to rationalize the plethora of traditional divisions, and clarify understanding, a revised scheme of lithostratigraphical classification for the Lias Group has recently been developed by the British Geological Survey (BGS) with the support of the Geological Society of London (Cox *et al.*, 1999) to divide the Lias Group into no more than 12 formations. The main outcrop has also been divided into four depositional areas - the Cleveland Basin, East Midlands Shelf (north and south), Worcester Basin (plus adjoining Bristol-

Radstock Shelf) and Wessex Basin (including parts of Somerset and south Wales). However, the fault-bounded Cardigan Bay Basin in west Wales contains the thickest onshore sequence of Lias mudstones in the UK at over 1300-m.

MATERIALS

Mudstone samples were predominantly collected from Lias Group outcrops in England together with borehole samples from Wales and the English Midlands (Figure 1). Quarries in Gloucestershire and Warwickshire and the Dorset coast were sampled to represent the Worcester Basin, Wessex Basin and southern part of the East Midlands Shelf. The Cleveland Basin was sampled from the Yorkshire coast between Staithes and Ravenscar (Table 1). Further details of the field sampling are given in Hobbs & Sumbler (2001).

Borehole samples were collected from the Lias sequence intercepted by the UK NIREX low-level radioactive waste site investigation at Fulbeck, Lincolnshire [SK 9062 5076] (Brandon *et al.*, 1990) and the IGS Llanbedr (Mochras Farm) Borehole, Gwynedd [SH 5533 2594], drilled in 1967 (Woodland, 1971). Samples were removed from the top, middle and base of the Lias succession of the Llanbedr Borehole in order to detect and assess any differences in their clay mineral assemblages (Table 1).

METHODS

The mineral assemblages and microtextures of the samples were investigated using X-ray diffraction (XRD), surface-area analyses, scanning electron (SEM) and transmission electron (TEM) microscopy. Further details of the analytical methodologies employed are given in Kemp & McKervey (2001) and Bouch (2003).

Representative portions of each sample were separated, dried at 55ºC and jawcrushed. Approximately ¼ of the jawcrushed material was then hammer-milled to pass a 125-µm screen for surface-area and whole-rock XRD analyses.

Surface-area determinations

Surface-area determinations were carried out following a procedure based on the formation of a monolayer of 2-ethoxyethanol (EGME) molecules on the clay surface under vacuum (Carter *et al.*, 1965).

X-ray diffraction

Whole-rock XRD analyses were carried out on micronised powders which were backloaded into a standard aluminium sample holders. <2-µm separates were isolated by gravity settling, then Ca-saturated, re-suspended and pipetted onto ceramic tiles in a vacuum apparatus to produce oriented mounts. XRD analysis was carried out using a Philips PW1700 series diffractometer fitted with a cobalt-target tube and operated at 45kV and 40mA. Whole-rock samples were scanned from 3-50 °2θ at 0.69 °2θ/minute. The <2-μm samples were scanned from 2-32 °2θ at 0.54 °2θ/minute as air-dry mounts, after glycol-solvation and after heating to 550°C for 2 hours. Diffraction data were firstly analysed using Philips X'Pert software coupled to an International Centre for Diffraction Data (ICDD) database.

Following identification of the mineral species present in the samples, mineral quantification was achieved using the Rietveld refinement technique (e.g. Snyder & Bish, 1989) using Siroquant v.2.5 software. This method avoids the need to produce synthetic mixtures and involves the least-squares fitting of measured to calculated XRD profiles using a crystal-structure databank. Hillier *et al.* (2001) quote errors for such an approach as typically ±2.5% for concentrations >60 wt%, ±5% for concentrations between 60 and 30 wt%, ±10% for concentrations between 30 and 10 wt%, ±20% for concentrations between 10 and 3 wt% and ±40% for concentrations <3 wt%.

In order to gain further information about the nature of the clay minerals present in the samples, modelling of the <2-μm XRD profiles was carried out using Newmod-for-Windows™ (Reynolds & Reynolds, 1996) software. Modelling was also used to assess the relative proportions of clay minerals present in the <2-μm fractions by comparison of sample XRD traces with Newmod-for-Windows™ modelled profiles following the method outlined in Moore & Reynolds (1997).

The relatively complex mineralogies of the Lias Group samples are difficult to quantify, even by employing state-of-the-art software modelling packages. For this reason the quoted mineral concentrations must be regarded with some caution. However, calculations using approximate values for %clay (from whole-rock XRD), the clay mineral concentrations from <2-µm XRD analysis and assuming theoretical surface-area values for the individual clay minerals, reveal similar whole-rock surface-area values to those determined empirically.

Scanning electron microscopy

For SEM analysis, centimetre-sized blocks of material were excavated from the central (i.e. least likely to be disturbed) portions of the hand-specimen samples, and were freeze- or air-dried. Once dried, a fresh fracture surface was prepared for each stub, with at least one fracture surface perpendicular to lamination prepared for each sample where possible. In addition to these fresh fracture surfaces, a number of samples also had surfaces prepared by cutting with a scalpel. Whilst this preparation disturbs the details of the structural relationships between the fine particles, it has the advantage of creating a relatively flat surface upon which compositional variations, as inferred from variations in back-scattered electron intensity (BSEM), are more apparent. The stubs were carbon-coated and analysed using a LEO 435VP digital SEM fitted with a KE Developments four-element solid-state backscattered electron detector, and an Oxford Instruments ISIS 300 EDXA system (for mineral identification by qualitative and semi-quantitative energy-dispersive X-ray analysis; EDXA).

Transmission electron microscopy

Prior to TEM observations, samples were treated with L. R. White resin following the procedures of Kim *et al.* (1995), in order to prevent collapse of smectite interlayers in the vacuum systems. Sticky-wax mounted thin sections were prepared with surfaces cut normal to bedding. Areas of interest were first imaged by SEM to locate the most appropriate areas for TEM observations. These areas, adhering to aluminium washers, were detached from thin sections, ion-milled and carbon-coated. TEM observations were made with a Philips CM12 TEM fitted with a scanning system and Kevex Quantum solid-state detector. The TEM was operated at 120 kV and a beam current of 20-µA. All high-resolution lattice-fringe images were obtained at 100,000x magnification. An objective aperture 20-µm in diameter was used for imaging. A camera length of 770-mm and a selected-area aperture 10-µm in diameter were used to obtain Selected Area Electron Diffraction (SAED) patterns.

RESULTS

Whole-rock mineral assemblages and surface-area

Thirteen different mineral phases were identified and quantified in the Lias Group samples (Table 2 and Figure 2). The presence of significant quantities of several different clay minerals and such complex mineralogies required many stages of refinement using the Siroquant software and resulted in mean chi-squared values of *c.*4.5. Chi-squared values of <3 indicate a well-refined pattern.

The Lias Group rocks are predominantly composed of quartz (5-52%, mean 28%), carbonates (calcite, dolomite and aragonite; nd-81%, mean 22%), 'clay' (undifferentiated mica species including muscovite, illite, I/S; kaolin, chlorite and smectite; 10-69%, mean 45%) and feldspar (albite and K-feldspar; nd-9%, mean 2%). The remaining minerals (pyrite, gypsum and jarosite) typically total <3% but may reach more elevated levels in selected samples.

From whole-rock XRD analysis (Figure 2), it is apparent that the samples from the East Midlands Shelf, the Cardigan Bay, Worcester and Wessex basins are more calcareous (nd-81%, mean 29%) than the Cleveland Basin samples which often contain no carbonate species or are only poorly calcareous (nd-24%, mean 3%). Dolomite is also more common in samples from the south (nd-14%, mean 2%) than in the north (nd-3%, mean 1%). Similarly the samples from the Wessex and Worcester basins and upper parts of the Cardigan Bay

Basin contain discrete smectite whereas I/S was detected in the East Midlands Shelf, Cleveland Basin and lowest Cardigan Bay Basin samples (see below).

The smectite-bearing samples from the Wessex, Worcester and Cardigan Bay basins have a mean surface-area of 110 m^2/g but a relatively large range of values from 27 to 203-m^2/g. Surface-areas for the I/S-bearing samples from the Cleveland Basin and East Midlands Shelf are generally smaller in comparison with a mean of 93-m^2/g and a range of 24 to 165-m^2/g (Figure 3).

Quartz contents are highest in the Cleveland Basin (24-47%, mean 33%), moderate in the Wessex (10-51%, mean 26%) and Worcester (6-52%, mean 30%) basins and low on the East Midlands Shelf (13-22%, mean 18%) and Cardigan Bay Basin (5-31%, mean 17%). Feldspar (predominantly albite) contents are typically low (mean 2%) but reach 9% in a few samples. K-feldspar is absent from the Cleveland and Worcester basins samples. Of the sulphur-bearing species, pyrite appears to be common (nd-6%, mean 2%) throughout the Lias Group whereas gypsum and jarosite occur sporadically but may form up to 12%.

SEM analyses indicate that the mudstones typically have well-laminated fabrics defined by the alignment of tightly-packed clay-mineral flakes. Individual flakes are typically <10-μm in diameter, and may have wispy outgrowths (Figure 4a, c). Minor authigenic framboidal pyrite is locally developed between clay flakes (Figure 4a, b), and gypsum/anhydrite is commonly observed on fracture and lamination surfaces. Samples from the

Cleveland Basin and East Midlands Shelf (north) contain relatively little carbonate which, where present, tends to occur in distinct veins. In contrast, samples from the East Midlands Shelf (south), Worcester Basin and Wessex Basin, in particular those from the Blue Lias Formation, commonly contain appreciable microcrystalline rhombs of calcite (and lesser amounts of dolomite) within the mudstone matrix, possibly representing recrystallised detrital carbonate (Figure 4d). Calcite veining ('Beef') is also common in Wessex Basin mudstones (particularly in the Charmouth Mudstone Formation).

Clay mineral assemblages

The Lias Group samples from the Cleveland Basin have similar clay mineral assemblages (Table 3, Figures 5 and 6a). Newmod-for-Windows modelling suggests that a typical <2-µm fraction is composed of 48% I/S, 27% illite, 19% kaolinite and 6% chlorite. However, modelling of the XRD traces is hindered by the almost complete overlap of peaks from different clay mineral species. For example, the modelling of chlorite is largely based on the d_{003} (4.73-Å) spacing as the d_{002} (7.1-Å) and d_{004} (3.54-Å) spacings are superimposed on the kaolinite d_{001} (7.1-Å) and d_{002} (3.58-Å) peaks. In addition to peak overlap problems, the broad peak profiles of the I/S leaves only d_{001} (*c.*11-Å) adequately resolved for modelling. The I/S component was therefore by necessity modelled using the diffraction trace of the air-dried sample.

Based on these limited data, modelling suggests that the I/S is 90% illite and 10% smectite R0 ordered interlayered clay, with a mean defect-free distance of 3 layers (10-Å units) and a size range of 1 to 15 layers. Illite has a mean defect-free distance of 7 layers and a size range of 1 to 28 layers. Chlorite was estimated to have similar mean defect-free distance of 7 layers (14-Å units) and a size range of 1 to 32 layers. Kaolinite has a mean defect-free distance of 11 layers (7-Å units) but a size range of 1 to 58 layers.

Clay mineral assemblages of samples from the north and south-western edge of the East Midlands Shelf (F187 and LGD1) are also comprised of I/S, illite, kaolinite and chlorite, and appear to have similar XRD characteristics to those from the Cleveland Basin (Table 3 and Figures 5 and 6b). However, the air-dry XRD profiles for the East Midlands Shelf samples indicates a subtle shift in the I/S d_{001} to *c.*12-Å, indicating an increase in the smectite component to perhaps 20%.

The very fine-grained clays forming the matrix of sample F187 (East Midlands Shelf, north) were imaged by TEM at magnifications in the range 50-140K. A series of lattice-fringe images indicate that the matrix clay minerals comprise approximately 85% mica (10-Å periodicity) with and without smectite interlayers, 10% kaolinite (7-Å periodicity) and 5% chlorite (14-Å periodicity). Although the clays are intergrown with authigenic calcite and pyrite, these non-clay minerals were not imaged.

Both detrital and authigenic micas are present in the matrix clay (Figure 7a). Relatively thick stacks of straight, sometimes mottled mica with typical thickness to length ratios of between 1:4 and 1:15 are probably detrital in origin (Figure 7b) and make up 10-15% of the clay micas. Within these detrital mica stacks, coherent 10-Å periodicity ranges from 5 to 64 layers and the main disruption of coherency is caused by layer terminations or single smectite layers (Figure 7c). One such mica image contains bands of reversed contrast normal to (00l), indicative of strain, and may have been derived from a metamorphic terrain. SAED patterns of detrital mica stacks show 2M polytypism but with diffuse or streaky 0*kl* layers parallel to *c**. Authigenic mica forms thin packets of 10-Å layers, typically 3 to 12 layers thick. Thicker packets tend to be straight whereas thinner ones may be slightly curved (Figure 7). SAED patterns of authigenic micas are concentric spotty rings, typical of a disordered $1M_d$ illite polytype. Authigenic illite is interlayered with smectite layers showing 11-12-Å periodicity, forming I/S. R1 ordering with a periodicity of approximately 21-Å is least common whereas R3 or R4 with periodicities of 33 or 44-Å are most common (Figure 7). The contrast between the ordering of I/S imaged by TEM and the R0 ordering indicated by XRD highlights two important differences in these techniques. Firstly, the <2-µm fraction analysed by XRD represents a disarticulated mudstone sample where some of the delicate crystals imaged by TEM have been broken down by the disaggregation technique (Li *et al*., 1998). Secondly, the X-ray beam has an averaging effect over a much larger area of sample, and includes more crystal defects and smectite interlayers than are apparent in the more restricted area of a TEM image.

Measurements were made of clay mica crystallite thicknesses by counting the number of coherent 10-Å fringes between smectite interlayers or other discontinuities, as described in Merriman *et al.* (1990) and Warr & Nieto (1998). The histogram shown in Figure 8 indicates a bimodal clay mica crystallite size distribution for the Lias sample from the East Midlands Shelf (north). The majority of measurements are from authigenic illite, which has a mean crystallite-size of 7 layers and a size range of approximately 1 to 30 (10-Å) units. In terms of reaction-progress these thicknesses indicate that the mudrocks are in the upper part of the Late Diagenetic Zone, equivalent to the light oil/wet gas zones of hydrocarbon maturity (Merriman & Kemp, 1996). A few measurements were also made on relatively large detrital micas that have a mean crystallite-size of 47 layers and an inferred size range of 35 to 70 (10-Å) units. Kaolinite and chlorite crystals have mean crystallite-sizes of 11 (7-Å) and 6 (14-Å) units respectively. These TEM measurements are in very close agreement to those deduced from Newmod-for-Windows modelling of XRD profiles.

The Lias samples from the Wessex and Worcester basins differ from their northern counterparts as they contain discrete smectite and no detectable I/S (Figures 5, 9a and b). Although they are otherwise similarly composed of illite, kaolinite and chlorite, they display a greater range of clay mineral concentrations. However, modelling suggests that a typical <2-μm fraction is composed of 37% illite, 26% smectite, 25% kaolinite and 11% chlorite. Modelling of the 'southern' sample XRD traces is similarly hindered by the almost complete overlap of peaks from different clay mineral species. In addition to peak overlap problems, the broad peak profiles of smectite, produced by its relatively small crystallite size, leaves only the d_{001} (17.0-Å) peak adequately resolved for modelling. Illite has a marginally greater mean defect-free distance of 9 layers and a size range of 1 to 35 (10-Å) units. Kaolinite and chlorite have approximately similar mean defect-free distances and size ranges to those models produced for the 'northern' samples. In comparison, smectite has a much smaller mean defect-free distance of 1.5 layers and a size range of only 1 to 5 (14.5-Å) units. Despite the problems involved in modelling the traces, 'realistic' modelled profiles were generated (Figure 10).

The clay mineral assemblages of the two shallower samples from the Llanbedr borehole are similar to but slightly more smectitic than those from the Wessex and Worcester basins. Size-distributions are also similar. However, the deepest sample is composed of 55% I/S (80% illite, air-dry I/S d_{001} *c*.12-Å), 35% illite, 4% kaolinite and 6% chlorite. Modelling indicates that the I/S shows similar characteristics to that identified in the East Midlands Shelf.

DISCUSSION

Mineral assemblages

The Lias Group samples, representing a wide geographic and stratigraphic range, have similar mineralogies to those described in previous studies (e.g. Deconinck *et al.*, 2003; Kemp & Hards, 1999; Mitchell, 1992; Bloodworth *et al.*, 1987; Pye & Krinsley, 1986; Cosgrove & Salter, 1966). Non-clay mineral assemblages are typically composed of carbonates (calcite, dolomite and aragonite), quartz, feldspar (albite and occasional K-feldspar), 'mica', pyrite, gypsum and jarosite. Clay mineral assemblages generally consist of illite, smectite or I/S, kaolinite and chlorite.

However, regional variations in mineralogy indicate that the Lias Group rocks of southern England and Wales (Wessex, Worcester and Cardigan Bay basins) and northern England (Cleveland Basin) have significantly different characteristics, whereas samples from the East Midlands Shelf share similar characteristics with both northern and southern samples.

The mudstones from southern England and Wales often contain large quantities of carbonate (principally as micro-rhombic and micritic calcite with minor dolomite and occasional aragonite) whereas those from northern England contain little or no carbonate. [The only sample from northern England to contain appreciable calcite is the silt/sandstone from the Staithes Sandstone Formation.]. The more calcareous nature of the southern mudstones and sandier nature of those in the north has been noted previously by Anderton *et al*. (1979).

The TEM images provide some insight into how the clay mineral assemblages in the Lias Group mudstones might have evolved. Early accumulations of calcareous mud probably contained a high proportion of smectite together with detrital flakes of mica and chlorite, and possibly kaolinite. In terms of provenance, the smectite may have been derived from more than one source, including pedogenic and volcanogenic clays; some smectite and kaolinite may have been neoformed within the basin (Pye & Krinsley, 1986). In contrast, detrital mica and chlorite were probably derived from a metamorphic terrain. As a result of burial, smectite has reacted to form illite, but the degree of replacement and the textures developed are variable. Thin illite crystals, generally <5 layers thick, occur in I/S where the wavy, anastomosing microfabric of the original smectite crystals is preserved. Thicker illite crystals, 5-15 layers thick, are straight with fewer layer terminations or other defects. The heterogeneity of detrital and authigenic clay minerals and textures is typical of mudrocks buried in an immature sedimentary basin (e.g. Hover *et al.*, 1996).

Maturity

Significant differences in the type and amount of swelling clay are found across the outcrop of the Lias Group mudstones. The Wessex and Worcester basins and shallower samples from the Cardigan Bay Basin contain discrete smectite whereas I/S (80-90% illite) is present in the East Midlands Shelf, Cleveland Basin and deepest sample from the Cardigan Bay Basin. Newmod-for-Windows modelling suggests that all the clay minerals present in the Lias Group have small mean defect-free distances, typically <10 layers thick. Such small crystallites are likely to provide an input from all clay species to the surface-area of the rock. However, the difference in the amount of swelling clay species does help to explain the slightly larger surface-area values for the southern samples (mean 110-m^2/g) compared with the northern samples (mean 93-m^2/g) despite a greater number of coarse-grained siltstone samples from the south. The apparent inverse relationship between surface-area and carbonate content is due to the dilution of the higher surface-area clay minerals by low surface-area carbonate minerals.

Regional differences in the type of swelling clay present also suggest differences in basin maturity and burial history. The most mature mudstones are from the Cleveland Basin where the presence of I/S (90% illite) suggests burial depths of perhaps 4-km, assuming a 'normal' geothermal gradient of 25-30°C/km (Merriman & Kemp, 1996). I/S (80% illite) in the sample from the East Midlands Shelf suggests shallower burial, perhaps to 3-km. Measurements of authigenic illite crystallite size in these two basins are consistent with a transition from immature to mature basins, equivalent to the oil window or top wet gas zone. However, the presence of smectite and kaolinite suggest that the mudstones from the Wessex and Worcester basins are immature and have been buried to depths of less than *c.*3-km, if the same geothermal gradient is assumed. The smectite to I/S transition demonstrated in the Cardigan Bay Basin suggests that the deepest Lias may have been buried to 3-km.

Vitrinite reflectance data for Middle Jurassic coals from the Cleveland Basin show reflectivities of *c.*0.85% and a rank equivalent to high volatile bituminous coals (Hemingway & Riddler, 1982). Barnard & Cooper (1983) used a combination of vitrinite reflectance and spore colouration indices to conclude that the Middle Jurassic had reached a maximum palaeotemperature of 95°C in the central part of the Cleveland Basin. Lower palaeotemperatures of *c.*80°C for the Middle Jurassic were obtained from fluid inclusion micro-thermometry from sphalerite grains (Hemingway & Riddler, 1982). Together these palaeotemperatures were taken to indicate a burial-depth of *c.*2.5-km for the base of the Middle Jurassic (Hemingway & Riddler, 1982). Adding 440-m of the Lias Group in the Cleveland Basin thus produces a maximum depth of burial of *c.*3-km. More recent and detailed modelling (Holliday, 1999) indicate that if the time of maximum burial was end-Cretaceous, then 2200-3000-m of Late Jurassic to Late Cretaceous strata have been removed from the main basin depocentre, assuming a lack of overpressuring. Alternatively if the time of maximum burial was mid-Cenozoic, the observed palaeotemperatures indicate that 2300-3200-m of Late Jurassic, Cretaceous and Palaeogene strata have been removed. Again, if the thickness of the Lias Group is added, a maximum depth of burial of *c.*4-km is indicated, in agreement with estimates based on clay reaction-progress data from this study. Hence a combination of clay mineral assemblages, sonic log studies and palaeotemperature assessments suggest that the observed elevated palaeotemperatures for the Cleveland Basin can be accounted for by deeper burial than hitherto estimated and, as suggested by Holliday (1999), there is no need to infer a local heating event.

As also discussed by Holliday (1999), there is only partial consensus between various modelling studies with regard to the thickness of the former overburden on the East Midlands Shelf. Estimates range from the 300-m obtained from sonic log measurements from the Cleethorpes Borehole (e.g. Kirby *et al.*, 1987) to 1700-m from converted apatite fission track palaeotemperatures (Green, 1989). If the maximum 850-m of removed Chalk favoured by Holliday (1999) and the Jurassic overburden estimate of 500-m (Dr M. Sumbler pers comm 2001) are accepted, this total depth of burial appears to disagree with the clay-derived 3-km of burial suggested in this study.

Subsidence history plots and hydrocarbon potential studies reveal much shallower depth of burial for the Lias Group in the Worcester and Wessex basins. Chadwick & Evans (1995) used mudstone densities to suggest that 1650-m of overburden had been removed from the Mercia Mudstone Group in the Kempsey borehole, south of Worcester whereas perhaps 1200-m had been removed from the eastern part of the basin. It would therefore appear that the Lias Group has only been buried to perhaps 1.5-km in the Worcester Basin.

Calculated organic maturity values of <0.50% R_0 (Ebukanson & Kinghorn, 1986) and organic geochemical analyses (Colter & Havard, 1981) for the Base Lias of the Wytch Farm oilfield, Dorset suggest organic immaturity. Although maturities are heavily influenced by the Purbeck-Isle of Wight Disturbance, burial-thermal history projections based on such data suggest a maximum burial of *c*.2-km and peak palaeotemperatures of *c*.75°C for the locations sampled in the Wessex Basin for this study. Clay mineral-based estimates of burial depth therefore appear reliable for the Worcester and Wessex basins. However, more recent T_{max} estimates of *c*.420°C for Dorset and *c*.430°C for Somerset from organic matter analyses (Deconinck *et al.*, 2003) suggest over-maturity. Even allowing for the faster reaction of organic matter to temperature, such data appears inconsistent with the clay mineral and stratigraphic model data.

CONCLUSIONS

This mineralogical study of a suite of Lias Group mudstones has generally confirmed the findings of previous workers. More importantly however, the wide geographic and stratigraphic distribution of the analysed samples has enabled a regional interpretation of the mineral assemblages and in particular clay mineral assemblages of the Lias Group in terms of its diagenetic and geological history and revealed that:

- Mudstones from southern England and Wales are often carbonate-rich while those from northern England contain little or no carbonate.

- The presence of I/S (90% illite) in the Cleveland Basin suggests a 4-km maximum depth of burial which corroborates earlier vitrinite reflectance-, fluid inclusion- and sonic velocity-based estimates.

- I/S (80% illite) detected from the East Midlands Shelf, suggests shallower burial to perhaps 3-km.

- Discrete smectite present in the Worcester and Wessex basins indicates even shallower burial to no more than 2-km.

- The >1300-m Lias Group present in the Cardigan Bay Basin reveals a transition from smectite in the upper and middle of the succession to I/S in its lower parts suggesting maximum burial of *c.*3-km.

ACKNOWLEDGEMENTS

The authors wish to thank John McKervey (BGS) for his assistance with mineralogical analysis. Peter Hobbs and Mike Sumbler (both BGS) are thanked for the field collection of many of the samples. TEM work was carried out during a visit to the University of Michigan, in collaboration with Don Peacor. The authors are grateful to Profs. Fernando Nieto and Don Peacor for their constructive reviews that improved this manuscript. This paper is published with the permission of the Executive Director, British Geological Survey (NERC).

REFERENCES

ANDERTON, R, BRIDGES, P H, LEEDER, M and SELLWOOD, B W. 1979. *A Dynamic Stratigraphy of the British Isles: A Study in Crustal Evolution.* George Allen & Unwin Ltd., London.

BARNARD, C E and COOPER, B S. 1983. A review of geochemical data related to the northwest European Gas Province. 19-33 in *Petroleum geochemistry and exploration of Europe*. BROOKS, J. (editor). Geological Society (London) and Blackwell Scientific Publishers, Oxford.

BESSA, J L and HESSELBO, S P. 1997. Gamma-ray character and correlation of the Lower Lias, SW Britain. *Proceedings of the Geologists' Association*, 108, 113-129.

BLOODWORTH, A J, KEMP, S J, INGLETHORPE, S D J and MORGAN, D J. 1987. Mineralogy and lithochemistry of strata beneath proposed low-level radioactive waste site at Fulbeck, Lincolnshire; Report to Sir Alexander Gibb and Partners, Site Investigation Consultants. *British Geological Survey Technical Report*, 87/15/C.

BOUCH, J E. 2003. SEM petrography of samples of the Lias Group of England and Wales. *British Geological Survey Technical Report*, IR/03/008.

BRANDON, A SUMBLER, M G AND IVEMEY-COOK, H C. 1990. A revised lithostratigraphy for the Lower and Middle Lias (Lower Jurassic) east of Nottingham, England. *Proceedings of the Yorkshire Geological Society*, 48, 121-141.

CARTER, D L, HEILMEN, M D & GONZALEZ, F L. 1965. Ethylene glycol monoethyl ether for determining surface area of silicate minerals. *Soil Science* 100, 356-360.

CHADWICK, R A and EVANS, C J. 1995. The timing and direction of Permo-Triassic extension in southern Britain. 161-192 in *Permian and Triassic rifting in Northwest Europe*. BOLDY, S A R. (editor). Geological Society Special Publication No. 91.

COLTER, V S and HAVARD, D J. 1981. The Wytch Farm oilfield, Dorset. 494-503 in *Petroleum Geology of the Continental Shelf of NW Europe*. ILLING, L V and HOBSON, D G. (editors). Hayden & Sons, London.

COSGROVE, M E and SALTER, D L. 1966. The stratigraphical distribution of kaolinite in the post-Armorican formations of South-West England. *Proceedings of the Ussher Society*, 1, 5, 249-252.

COX, B M, SUMBLER, M G and IVIMEY-COOK, H C. 1999. A formational framework for the Lower Jurassic of England and Wales (Onshore Area). *British Geological Survey Research Report*, RR/99/01.

DECONINCK, J F, HESSELBO, S P, DEBUISSER, N, AVERBUCH, O, BAUDIN, F and BESSA, J. 2003. Environmental controls on clay mineralogy of an Early Jurassic mudrock (Blue Lias Formation, southern England). *International Journal of Earth Science*, 92, 255-266.

EBUKANSON, E J and KINGHORN, R R F. 1986. Maturity of organic matter in the Jurassic of southern England and its relation to the burial history of the sediments. *Journal of Petroleum Geology*, 9, 259-280.

GREEN, P F. 1989. Thermal and tectonic history of the East Midlands shelf (onshore UK) and surrounding regions assessed by apatite fission track analysis. *Journal of the Geological Society (London)*, 146, 755-773.

HALLAM, A. 1960. A sedimentary and faunal study of the Blue Lias of Dorset and Glamorgan. *Philosophical Transactions of the Royal Society*, B243, 698, 1-44.

HEMINGWAY, J E and RIDDLER, G P. 1982. Basin inversion in North Yorkshire. *Transactions of the Institution of Mining & Metallurgy*, B91, 175-186.

HILLIER, S, SUZUKI, K and COTTER-HOWELLS, J. 2001. Quantitative determination of Cerussite (lead carbonate) by X-ray powder diffraction and inferences for lead speciation and transport in stream sediments from a former lead mining area of Scotland. *Applied Geochemistry*, 16, 597-608.

HOBBS, P R N and SUMBLER, M. 2001. Field sampling visits to Lias locations on the Yorkshire and Dorset coasts and elsewhere (October & November, 2000). *British Geological Survey Internal Report*, IR/01/71.

HOLLIDAY, D W. 1999. Palaeotemperatures, thermal modelling and depth of burial studies in northern and eastern England. *Proceedings of the Yorkshire Geological Society*, 52 (4), 337-352.

HOVER, V C, PEACOR, D R, and WALKER, L M. 1996. STEM/AEM evidence for preservation of burial diagenetic fabrics in Devonian shales: implications for fluid/rock interactions in cratonic basins (U.S.A.) *Journal of Sedimentary Research*, 66**,** 519-530.

HOWER, J, ESLINGER, E V, HOWER, M E and PERRY, E A. 1976. Mechanism of burial metamorphism of argillaceous sediments: Mineralogical and chemical evidence. *Geological Society of America Bulletin*, 87, 725-737.

KEMP, S J and HARDS, V L. 2000. The mineralogy of Lower Jurassic (Lias) mudstones from the M5, Gloucestershire. *British Geological Survey Technical Report,* WG/00/11.

KEMP, S J and MCKERVEY, J A. 2001. The mineralogy of mudrocks from the Lias Group of England. *British Geological Survey Technical Report*, IR/01/124.

KIM, J-W, PEACOR, D R, TESSIER, D and ELSASS, F. 1995. A technique for maintaining texture and permanent expansion of smectite interlayers for TEM observations. *Clays and Clay Minerals,* 43, 51-57.

KIRBY, G A, SMITH, K, SMITH, N J P and SWALLOW, P W. 1987. Oil and gas generation in eastern England. In: Brooks, J & Glennie, K W (eds) *Petroleum Geology of North West Europe,* Volume 1, Graham & Trotman, London, 171-180.

LI, G, PEACOR, D R, BUSECK, P R and ÁRKAI, P. 1998. Modification of illite-muscovite crystallite-size distributions by sample preparation for powder XRD analysis. *Canadian Mineralogist*, 36, 1435-1451.

MITCHELL, C J. 1992. Clay mineralogy of the Lias, Copperhill Quarry, Grantham. *British Geological Survey Technical Report*, WG/92/9.

MERRIMAN, R J and KEMP, S J. 1996. Clay minerals and sedimentary basin maturity. *Mineralogical Society Bulletin*, 111, 7-8.

MERRIMAN, R J and FREY, M. 1999. Patterns of very low-grade metamorphism in metapelitic rocks. In: Frey, M & Robinson, D. (eds) *Low-Grade Metamorphism.* Blackwell Sciences Ltd., Oxford., pp 61-107.

MERRIMAN, R J and PEACOR, D R. 1999. Very low-grade metapelites; mineralogy, microfabrics and measuring reaction progress. In: Frey, M & Robinson, D. (eds) *Low-Grade Metamorphism.* Blackwell Sciences Ltd., Oxford., pp 10-60.

MERRIMAN, R J, ROBERTS, B and PEACOR, D R. 1990. A transmission electron microscope study of white mica crystallite size distribution in a mudstone to slate transitional sequence, North Wales, U.K. *Contributions to Mineralogy and Petrology*, 106, 27-40.

MOORE, D M and REYNOLDS, R C. 1997. *X-Ray Diffraction and the Identification and Analysis of Clay Minerals, Second Edition.* Oxford University Press, New York.

POTTER, P E, MAYNARD, J B and PRYOR, W A. 1980. *Sedimentology of Shale*, Springer-Verlag, Berlin, pp270.

PYE, K and KRINSLEY, D H. 1986. Microfabric, mineralogy and early diagenetic history of the Whitby Mudstone Formation (Toarcian), Cleveland Basin, UK. *Geological Magazine*, 123, 191-203.

REYNOLDS, R C and REYNOLDS, R C. 1996. *Description of Newmod-for-Windows™. The calculation of one-dimensional X-ray diffraction patterns of mixed layered clay minerals*. R C Reynolds Jr., 8 Brook Road, Hanover, NH.

SNYDER, R L and BISH, D L. 1989. Quantitative analysis. In: Bish, D.L., Post, J.E. (Eds), *Modern Powder Diffraction, Reviews in Mineralogy*, Volume 20, Mineralogical Society of America, USA, pp. 101-144 (Chapter 5).

VAN BUCHEM, F S P, MELNYK, D H and MCCAVE, I N. 1992. Chemical cyclicity and correlation of Lower Lias mudstones using gamma ray logs, Yorkshire, UK. *Journal of the Geological Society*, 149, 991-1002.

WARR, L N and NIETO, F. 1998. Crystallite thickness and defect density of Phyllosilicates in low-temperature metamorphic pelites: A TEM and XRD study of clay-mineral crystallinity-index standards. *The Canadian Mineralogist*, 36, 1353-1474.

WOODLAND, A W. 1971. The Llanbedr (Mochras Farm) borehole. *Report of the Institute of Geological Sciences no. 71/18.*

Table 1.

Sample No.	Location (including depth for bh samples)	NGR	Basin	Stratigraphy		Description
				Formation	Member (zone)	
LGD1	Harbury, Warwickshire (qy)	SP 3862 5880	E. Mids. Shelf (south)	Blue Lias	Rugby Limestone	Dark grey mudstone with shell fragments
F187	Fulbeck, Lincolnshire (bh), 82.1 m	SK 9062 5076	E. Mids. Shelf (north)	Scunthorpe Mudstone	N/A	Medium grey, laminated mudstone
H065	Llanbedr, (Mochras Farm), Gwynedd (bh), 622.7 m	SH 5533 2594	Cardigan Bay	unknown	unknown	Pale grey, calcareous, silty mudstone
H066	Llanbedr, (Mochras Farm), Gwynedd (bh), 1317.0 m	SH 5533 2594	Cardigan Bay	unknown	unknown	Medium grey, calcareous mudstone
H067	Llanbedr, (Mochras Farm), Gwynedd (bh), 1906.5 m	SH 5533 2594	Cardigan Bay	unknown	unknown	Dark grey, 'paper shale', calcareous mudstone
LGD2	Northcot, Blockley, Gloucester (qy)	SP 1795 3699	Worcester	Charmouth Mudstone	N/A	Dark grey mudstone with shell fragments.
LGD3	Northcot, Blockley, Gloucester (qy)	SP 1803 3404	Worcester	Charmouth Mudstone	N/A	Dark grey mudstone with shell fragments
LGD11A	Robins Wood Hill, Gloucester (qy)	SO 835 149	Worcester	Whitby Mudstone	N/A	Green mudstone with black 'root-like' material
LGD11B	Robins Wood Hill, Gloucester (qy)	SO 835 149	Worcester	Whitby Mudstone	N/A	Pale green siltstone
LGD12	Robins Wood Hill, Gloucester (qy)	SO 835 149	Worcester	Dyrham	N/A	Dark grey, laminated mudstone with shell fragments
LGD4	Ware Cliff, Lyme Regis, Dorset (ct)	SY 3315 9138	Wessex	Blue Lias	(Angulata zone)	Dark grey, laminated mudstone
LGD5	Ware Cliff, Lyme Regis, Dorset (ct)	SY 3337 9154	Wessex	Charmouth Mudstone	Shales-with-Beef	Dark/pale grey, laminated mudstone
LGD6	Stonebarrow Hill, Dorset (ct)	SY 3816 9264	Wessex	Charmouth Mudstone	Belemnite Marl	Medium grey siltstone
LGD7	Cain's Folly, Stonebarrow Hill, Dorset (ct)	SY 3739 9288	Wessex	Charmouth Mudstone	Black Ven Marl	Dark grey mudstone with shell fragments
LGD8	Cain's Folly, Stonebarrow Hill, Dorset (ct)	SY 3739 9288	Wessex	Charmouth Mudstone	Black Ven Marl	Dark grey, laminated mudstone
LGD9	Seatown, Dorset (ct)	SY 4221 9162	Wessex	Dyrham	Eype Clay	Medium-dark grey mudstone
LGD10	Watton Cliff, Dorset (ct)	SY 4529 9094	Wessex	Bridport Sand	Down Cliff Clay	Green siltstone
LGD13	Ravenscar (golf course), N. Yorkshire	NZ 9799 0173	Cleveland	Whitby Mudstone	Alum Shale	Dark grey, laminated mudstone
LGD14	Ravenscar (golf course), N. Yorkshire	NZ 9829 0211	Cleveland	Whitby Mudstone	Mulgrave Shale	Dark grey, laminated mudstone, fossil fragments
LGD15	Ravenscar, N. Yorkshire	NZ 9778 0223	Cleveland	Redcar Mudstone	Pyritous Shale (lower)	Medium to dark grey, laminated mudstone
LGD16	Staithes, N. Yorkshire	NZ 7880 1886	Cleveland	Cleveland Ironstone	3m below Avicula seam	Dark grey, laminated mudstone
LGD17	Staithes, N. Yorkshire	NZ 78565 18879	Cleveland	Staithes Sandstone	N/A	Pale/medium grey, massive silt/sandstone, fossil fragments
LGD18	Runswick Bay, N. Yorkshire (ct)		Cleveland	Whitby Mudstone	Mulgrave Shale	Dark grey, laminated mudstone, oxidised pyrite
LGD19	Kettleness, N. Yorkshire (ct)	NZ 8318 1603	Cleveland	Whitby Mudstone	Grey Shales	Dark grey, laminated mudstone
LGD20	Kettleness, N. Yorkshire (ct)	NZ 8317 1599	Cleveland	Whitby Mudstone	Grey Shales	Dark grey, laminated mudstone
LGD21	Kettleness, N. Yorkshire (former alum qy)	NZ 8346 1586	Cleveland	Whitby Mudstone	Alum Shale	Dark grey, laminated mudstone, oxidised pyrite
LGD22	Kettleness, N. Yorkshire (former alum qy)	NZ 8321 1603	Cleveland	Whitby Mudstone	Mulgrave Shale	Dark grey, laminated mudstone
LGD23	Robin Hood's Bay, N. Yorkshire (harbour)		Cleveland	Redcar Mudstone	Ironstone Shale	Dark grey, laminated mudstone
LGD24	Boggle Hole, N. Yorkshire	NZ 9644 0313	Cleveland	Redcar Mudstone	Calcareous Shales (upper)	Medium grey, laminated mudstone
LGD25	Boggle Hole, N. Yorkshire	NZ 9631 0307	Cleveland	Redcar Mudstone	Calcareous Shales (lower)	Dark grey, laminated mudstone

KEY: (qy) quarry, (bh) borehole, (ct) coast, N/A not available.

Table 2.

Sample No.	**Location**	**Basin**	**%mineral**														**Surface-area**
			quartz	**calcite**	**pyrite**	**dolomite**	**'mica'**	**K-feld.**	**kaolin**	**chlorite**	**smectite**	**albite**	**gypsum**	**jarosite**	**aragonite**	**I/S**	**m^2/g**
LGD1	Harbury, Warks. (qy)	E. Mids. Shelf (south)	22	47	2	1	20	nd	4	nd	nd	1	nd	nd	nd	3	114
F187	Fulbeck, Lincolnshire (borehole)	E. Mids. Shelf (north)	13	11	2	nd	36	2	25	nd	nd	2	nd	1	nd	8	165
H065	Llanbedr, (Mochras Farm), Gwynedd (bh)	Cardigan Bay	31	37	2	1	13	3	9	nd	2	2	nd	nd	nd	nd	80
H066	Llanbedr, (Mochras Farm), Gwynedd (bh)	Cardigan Bay	5	76	2	1	5	2	6	nd	1	1	nd	nd	1	nd	44
H067	Llanbedr, (Mochras Farm), Gwynedd (bh)	Cardigan Bay	15	26	3	2	33	1	2	nd	nd	2	nd	nd	6	10	110
LGD2	Northcot, Blockley, Gloucs.(qy)	Worcester	52	1	1	nd	22	nd	20	nd	1	3	nd	nd	nd	nd	86
LGD3	Northcot, Blockley, Gloucs.(qy)	Worcester	38	1	1	nd	39	nd	21	nd	nd	nd	nd	nd	nd	nd	97
LGD11A	Robins Wood Hill, Gloucester (qy)	Worcester	12	69	nd	nd	15	nd	4	nd	nd	nd	nd	nd	nd	nd	77
LGD11B	Robins Wood Hill, Gloucester (qy)	Worcester	6	81	nd	nd	8	nd	2	nd	nd	nd	1	2	nd	nd	27
LGD12	Robins Wood Hill, Gloucester (qy)	Worcester	40	nd	1	nd	29	nd	22	nd	3	3	2	nd	nd	nd	116
LGD4	Ware Cliff, Lyme Regis, Dorset (ct)	Wessex	13	51	4	5	22	nd	2	nd	nd	nd	3	nd	nd	nd	137
LGD5	Ware Cliff, Lyme Regis, Dorset (ct)	Wessex	22	20	5	1	31	1	9	nd	2	nd	8	1	nd	nd	203
LGD6	Stonebarrow Hill, Dorset (ct)	Wessex	10	56	2	12	17	nd	2	nd	nd	1	nd	nd	nd	nd	77
LGD7	Cain's Folly, Stonebarrow Hill, Dorset (ct)	Wessex	22	27	4	4	33	nd	10	nd	nd	nd	nd	nd	nd	nd	123
LGD8	Cain's Folly, Stonebarrow Hill, Dorset (ct)	Wessex	17	23	6	14	33	nd	6	nd	nd	nd	1	nd	nd	nd	179
LGD9	Seatown, Dorset (ct)	Wessex	44	3	1	nd	28	nd	15	nd	2	7	nd	nd	nd	nd	98
LGD10	Watton Cliff, Dorset (ct)	Wessex	51	21	nd	nd	17	1	5	nd	2	3	nd	nd	nd	nd	106
LGD13	Ravenscar (golf course), N. Yorkshire	Cleveland	30	nd	5	nd	42	nd	21	nd	nd	nd	nd	nd	nd	2	96
LGD14	Ravenscar (golf course), N. Yorkshire	Cleveland	28	3	6	nd	38	nd	21	nd	nd	nd	nd	nd	nd	4	85
LGD15	Ravenscar, N. Yorkshire	Cleveland	29	8	3	nd	37	nd	21	nd	nd	nd	nd	nd	nd	2	86
LGD16	Staithes, N. Yorkshire	Cleveland	36	nd	2	nd	36	nd	17	nd	nd	7	nd	nd	nd	2	66
LGD17	Staithes, N. Yorkshire	Cleveland	40	24	1	3	13	nd	10	nd	nd	9	nd	nd	nd	nd	24
LGD18	Runswick Bay, N. Yorkshire (ct)	Cleveland	25	nd	3	nd	28	nd	10	nd	nd	1	10	12	nd	11	78
LGD19	Kettleness, N. Yorkshire (ct)	Cleveland	39	nd	3	nd	31	nd	21	nd	nd	4	nd	nd	nd	2	66
LGD20	Kettleness, N. Yorkshire (ct)	Cleveland	31	nd	2	nd	40	nd	18	nd	nd	nd	nd	nd	nd	9	96
LGD21	Kettleness, N. Yorkshire (former alum qy)	Cleveland	32	nd	nd	nd	38	nd	20	nd	nd	nd	nd	nd	nd	10	134
LGD22	Kettleness, N. Yorkshire (former alum qy)	Cleveland	24	nd	1	nd	36	nd	17	nd	nd	nd	8	4	nd	10	117
LGD23	Robin Hood's Bay, N. Yorkshire (harbour)	Cleveland	24	6	2	nd	42	nd	21	1	nd	nd	1	nd		3	100
LGD24	Boggle Hole, N. Yorkshire	Cleveland	38	1	1	3	37	nd	17	nd	nd	1	nd	nd		2	79
LGD25	Boggle Hole, N. Yorkshire	Cleveland	47	nd	nd	1	32	nd	15	nd	nd	1	nd	nd		4	76

KEY: (qy) quarry, (bh) borehole, (ct) coast, nd not detected

Table 3.

Sample No.	Location	Basin	%clay mineral				
			smectite	I/S	illite	chlorite	kaolinite
LGD1	Harbury, Warks. (qy)	E. Mids. Shelf (south)	nd	22	50	10	18
F187	Fulbeck, Lincolnshire (borehole)	E. Mids. Shelf (north)	nd	30	29	13	28
H065	Llanbedr, (Mochras Farm), Gwynedd (bh)	Cardigan Bay	49	nd	38	5	9
H066	Llanbedr, (Mochras Farm), Gwynedd (bh)	Cardigan Bay	40	nd	42	6	12
H067	Llanbedr, (Mochras Farm), Gwynedd (bh)	Cardigan Bay	nd	55	35	6	4
LGD2	Northcot, Blockley, Gloucs.(qy)	Worcester	15	nd	23	18	43
LGD3	Northcot, Blockley, Gloucs.(qy)	Worcester	11	nd	27	17	45
LGD11A	Robins Wood Hill, Gloucester (qy)	Worcester	30	nd	48	5	16
LGD11B	Robins Wood Hill, Gloucester (qy)	Worcester	21	nd	56	5	17
LGD12	Robins Wood Hill, Gloucester (qy)	Worcester	26	nd	19	17	38
LGD4	Ware Cliff, Lyme Regis, Dorset (ct)	Wessex	16	nd	60	8	16
LGD5	Ware Cliff, Lyme Regis, Dorset (ct)	Wessex	36	nd	29	10	24
LGD6	Stonebarrow Hill, Dorset (ct)	Wessex	18	nd	66	5	11
LGD7	Cain's Folly, Stonebarrow Hill, Dorset (ct)	Wessex	18	nd	38	17	27
LGD8	Cain's Folly, Stonebarrow Hill, Dorset (ct)	Wessex	30	nd	32	11	27
LGD9	Seatown, Dorset (ct)	Wessex	37	nd	17	17	29
LGD10	Watton Cliff, Dorset (ct)	Wessex	71	nd	12	2	15
LGD13	Ravenscar (golf course), N. Yorkshire	Cleveland	nd	52	23	6	19
LGD14	Ravenscar (golf course), N. Yorkshire	Cleveland	nd	45	29	5	21
LGD15	Ravenscar, N. Yorkshire	Cleveland	nd	55	21	5	18
LGD16	Staithes, N. Yorkshire	Cleveland	nd	42	29	10	19
LGD17	Staithes, N. Yorkshire	Cleveland	nd	42	25	13	21
LGD18	Runswick Bay, N. Yorkshire (ct)	Cleveland	nd	36	40	4	20
LGD19	Kettleness, N. Yorkshire (ct)	Cleveland	nd	49	28	5	18
LGD20	Kettleness, N. Yorkshire (ct)	Cleveland	nd	56	26	4	14
LGD21	Kettleness, N. Yorkshire (former alum qy)	Cleveland	nd	48	27	4	20
LGD22	Kettleness, N. Yorkshire (former alum qy)	Cleveland	nd	54	21	4	21
LGD23	Robin Hood's Bay, N. Yorkshire (harbour)	Cleveland	nd	46	25	6	24
LGD24	Boggle Hole, N. Yorkshire	Cleveland	nd	45	31	7	17
LGD25	Boggle Hole, N. Yorkshire	Cleveland	nd	51	31	5	13

KEY: (qy) quarry, (bh) borehole, (ct) coast, nd not detected

TABLES AND FIGURES

Table 1. Summary of samples.

Table 2. Summary of whole-rock X-ray diffraction and surface-area (S.A.) analyses.

Table 3. Summary of <2-µm clay mineral X-ray diffraction analyses.

Figure 1. Location map showing the study sites, the generalised outcrop of the Lias Group in England and Wales and the structural elements that controlled deposition.

Figure 2. The whole-rock mineral assemblages of the Lias Group samples.

Figure 3. The surface-area of the Lias Group samples.

Figure 4. Scanning electron micrographs showing typical features of Lias Group mudstones. (a) Tightly packed, flat-lying, curved clay flakes, typically approximately 10-µm in diameter and <1-µm thick. Minor framboidal pyrite is present near the bottom of the image (Whitby Mudstone Formation, Cleveland Basin). (b) A cluster of pyrite framboids within a microfracture that cuts an otherwise well-laminated mudstone (Charmouth Mudstone Formation, East Midlands Shelf (north)). (c) Well-laminated, tightly packed, flat lying clay flakes with minor silt-sized grains (Blue Lias Formation, Worcester Basin). (d) Carbonate-rich mudstone containing very

abundant, microcrystalline rhombs of calcite (A). A pyrite framboid is engulfed by authigenic clay at (B). (Blue Lias Formation, Wessex Basin).

Figure 5. The clay mineral assemblages of the Lias Group samples.

Figure 6. Representative X-ray diffraction traces of <2-µm separates, (a) Redcar Mudstone Formation, Cleveland Basin, (b) Blue Lias Formation, East Midland Shelf.

Figure 7. Transmission electron micrographs showing typical features of Lias Group mudstones. (a) Low-magnification image showing authigenic clay minerals kaolinite (Ka) and illite/smectite (I/S). Authigenic pyrite (Py) and a detrital quartz grain (Qz) are also present. Width of field is 0.5-µm. (b) Lattice-fringe image of a mottled detrital mica (DM) enclosed in thin crystals of illite (I) and illite/smectite (I/S). (c) Inset from (b) showing a thick stack of 10Å fringes in the detrital mica (DM), compared with 10-Å fringes in thin illite. I/S shows 10-Å fringes of illite interlayered with 11-12Å fringes of smectite. (d) Lattice-fringe image of thin illite/smectite crystals with R=2 and R=3 ordering, and also a few discrete smectite crystals 2 or 3 layers thick; I=10Å; S=11-12Å. Sample F187, East Midlands Shelf (north).

Figure 8. Clay mica crystallite-size distribution, sample F187, East Midlands Shelf (north). The size distribution is bimodal, with a mean[1] for authigenic illite at 7.1 (x10Å units), and mean[2] of 46.5 (x10Å units) for detrital mica.

Figure 9. Representative X-ray diffraction traces of <2-μm separates, (a) Charmouth Mudstone Formation, Wessex Basin, (b) Dyrham Formation, Worcester Basin.

Figure 10. Example of experimental and NEWMOD-modelled XRD profiles. Ethylene glycol-solvated <2-μm oriented mount, sample LGD10, Watton Cliff, Dorset.

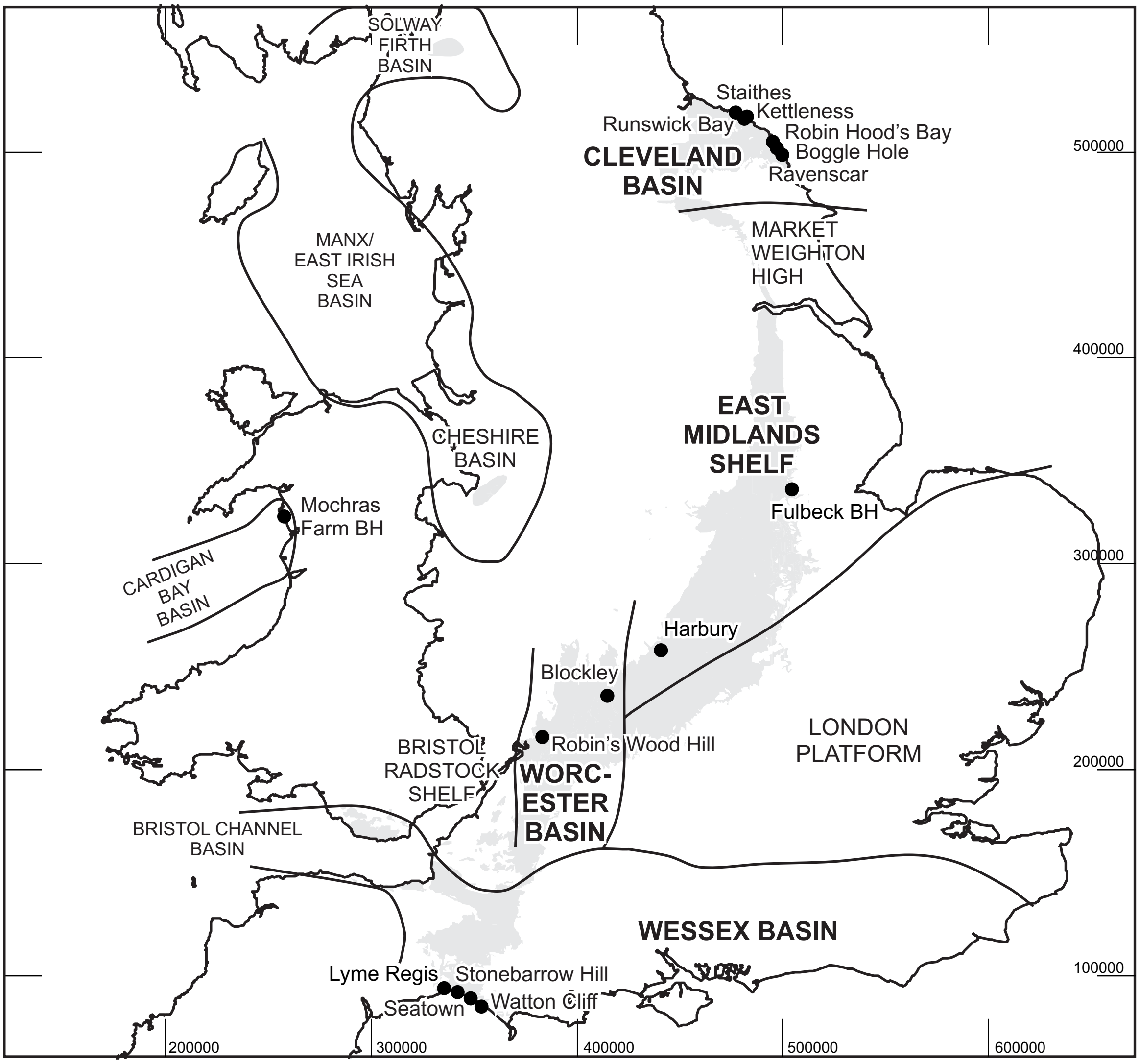

● Study Sites Lias deposits at surface Positions of basins and shelves from Cox *et al.* (1999)

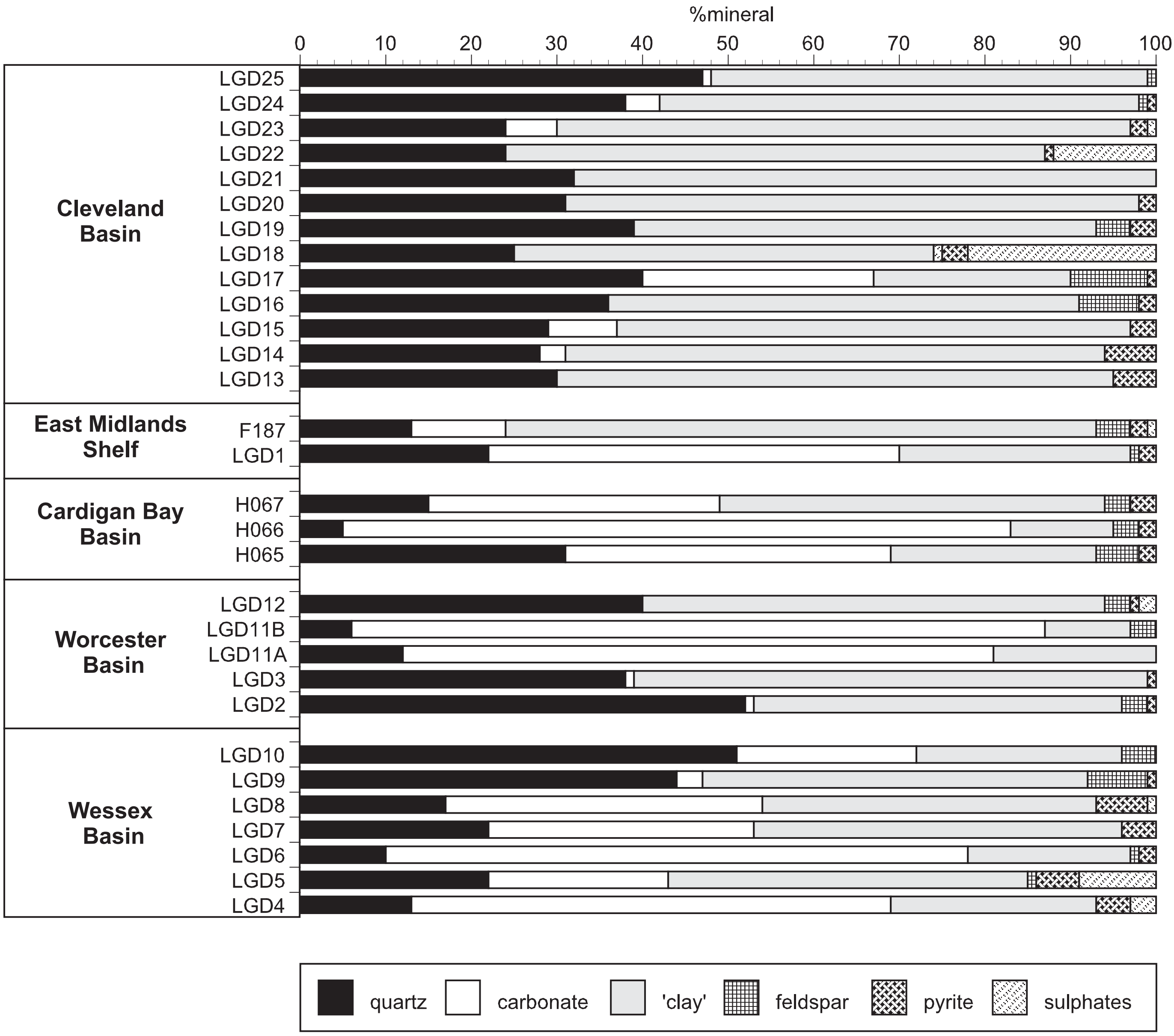
%mineral
0
10
20
30
40
50
60
70
80
90
100
Cleveland Basin
LGD25
LGD24
LGD23
LGD22
LGD21
LGD20
LGD19
LGD18
LGD17
LGD16
LGD15
LGD14
LGD13
East Midlands Shelf
F187
LGD1
Cardigan Bay Basin
H067
H066
H065
Worcester Basin
LGD12
LGD11B
LGD11A
LGD3
LGD2
Wessex Basin
LGD10
LGD9
LGD8
LGD7
LGD6
LGD5
LGD4
quartz
carbonate
'clay'
feldspar
pyrite
sulphates

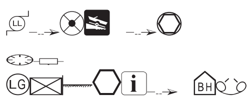

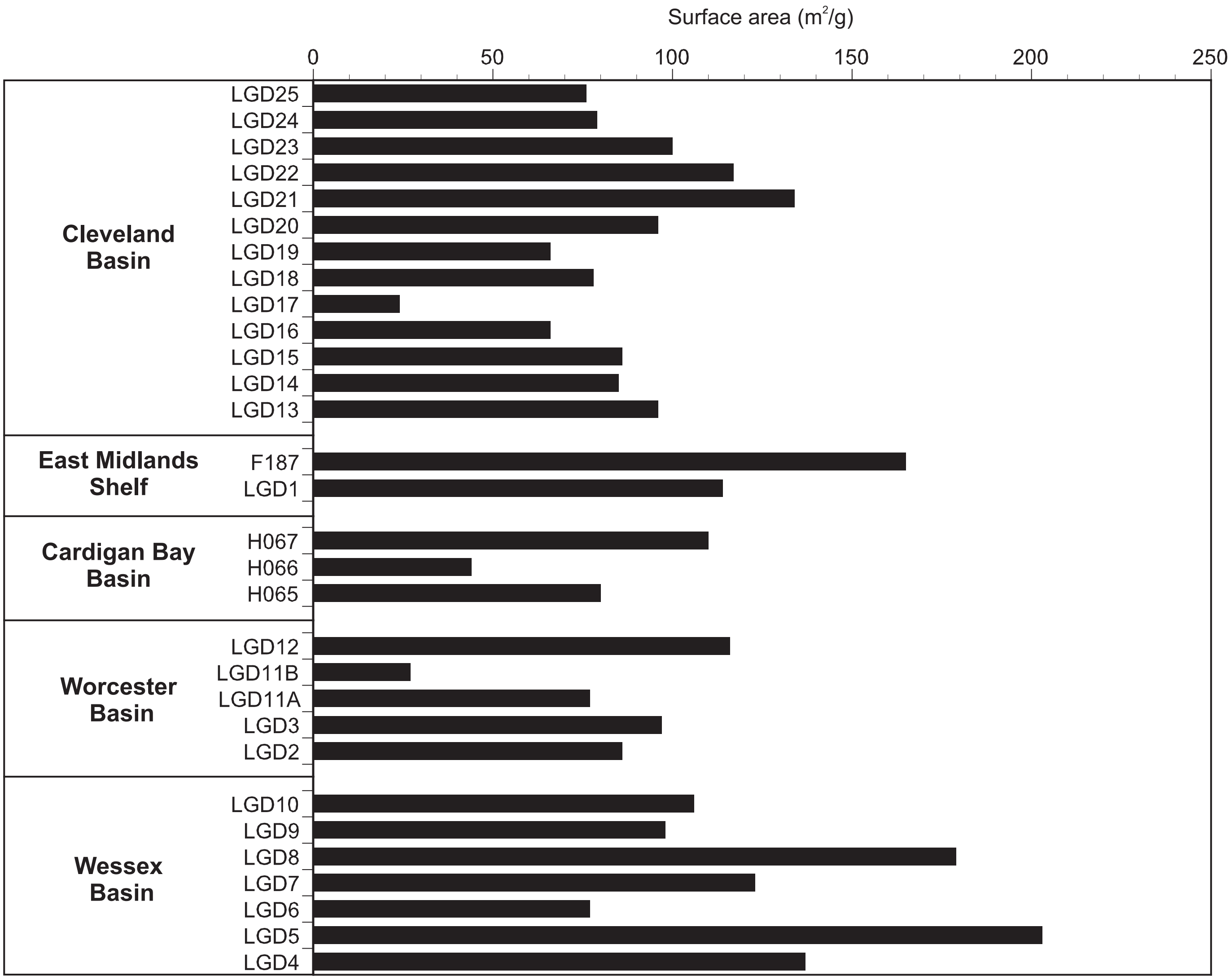
Surface area (m^2/g)
0
50
100
150
200
250
Cleveland Basin
LGD25
LGD24
LGD23
LGD22
LGD21
LGD20
LGD19
LGD18
LGD17
LGD16
LGD15
LGD14
LGD13
East Midlands Shelf
F187
LGD1
Cardigan Bay Basin
H067
H066
H065
Worcester Basin
LGD12
LGD11B
LGD11A
LGD3
LGD2
Wessex Basin
LGD10
LGD9
LGD8
LGD7
LGD6
LGD5
LGD4

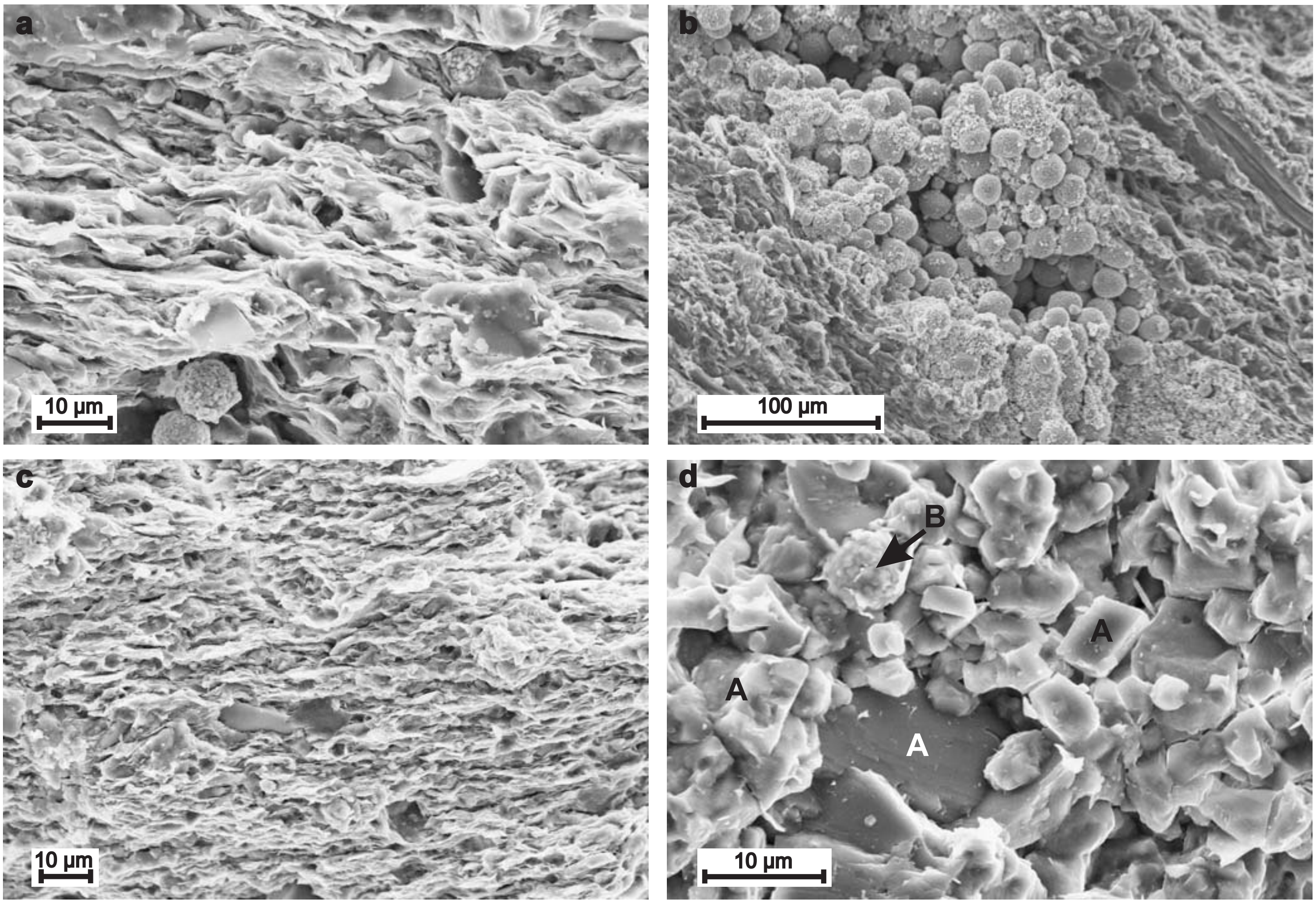
a
10 µm
b
100 µm
c
10 µm
d
B
A
A
A
10 µm

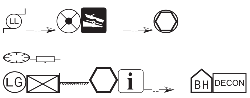
LG
i
BH
DECON

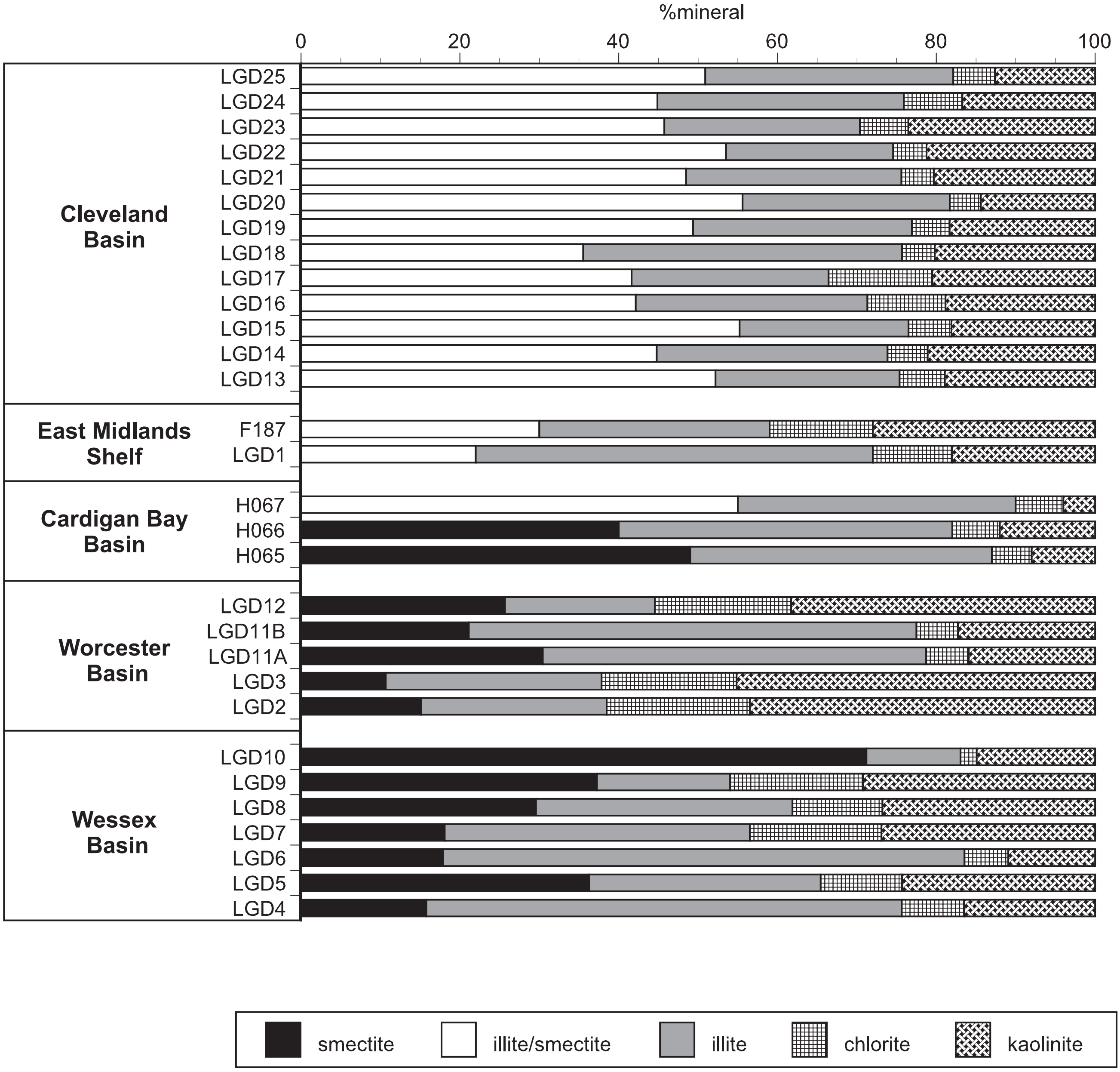

%mineral
0
20
40
60
80
100
Cleveland Basin
LGD25
LGD24
LGD23
LGD22
LGD21
LGD20
LGD19
LGD18
LGD17
LGD16
LGD15
LGD14
LGD13
East Midlands Shelf
F187
LGD1
Cardigan Bay Basin
H067
H066
H065
Worcester Basin
LGD12
LGD11B
LGD11A
LGD3
LGD2
Wessex Basin
LGD10
LGD9
LGD8
LGD7
LGD6
LGD5
LGD4
smectite
illite/smectite
illite
chlorite
kaolinite

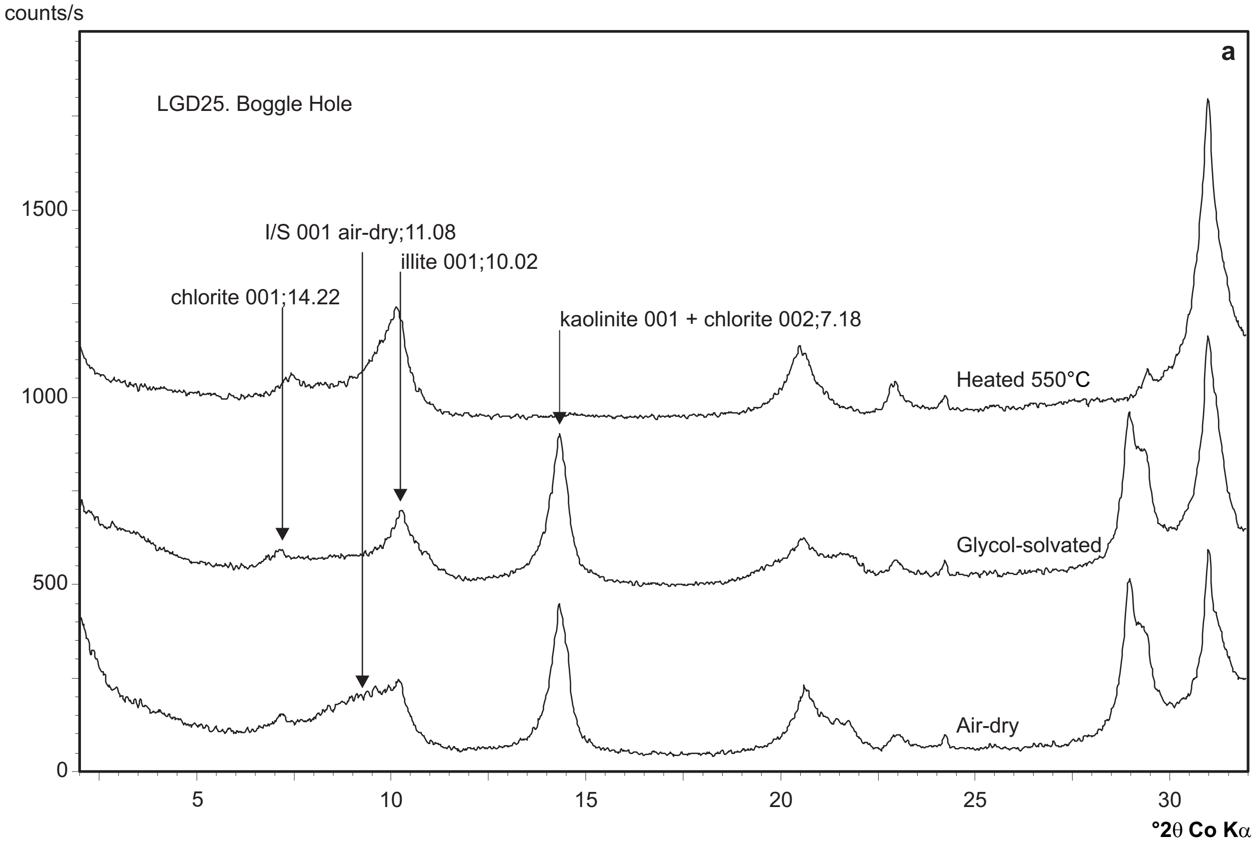
counts/s
a
LGD25. Boggle Hole
1500
1000
500
0
I/S 001 air-dry;11.08
illite 001;10.02
chlorite 001;14.22
kaolinite 001 + chlorite 002;7.18
Heated 550°C
Glycol-solvated
Air-dry
5
10
15
20
25
30
°2θ Co Kα

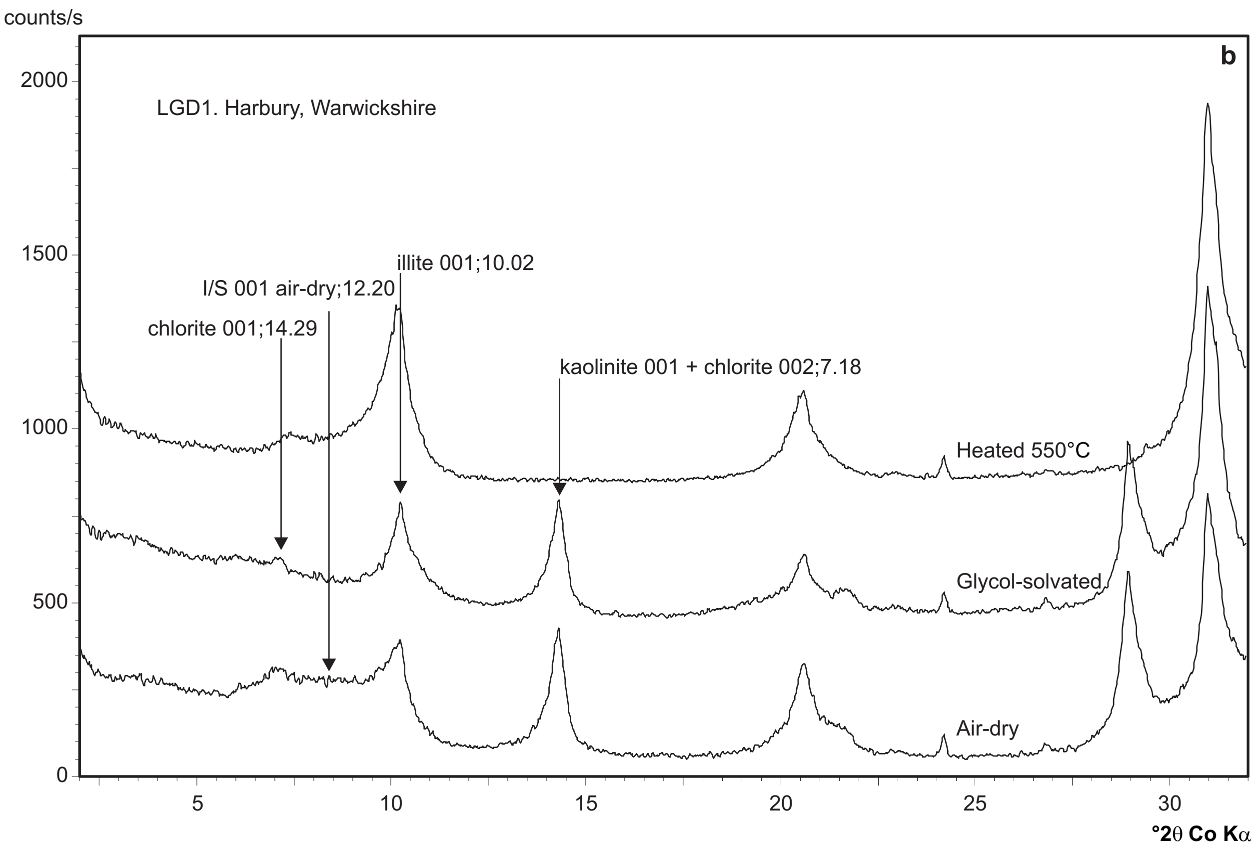
counts/s
b
2000
LGD1. Harbury, Warwickshire
1500
1000
500
0
illite 001;10.02
I/S 001 air-dry;12.20
chlorite 001;14.29
kaolinite 001 + chlorite 002;7.18
Heated 550°C
Glycol-solvated
Air-dry
5
10
15
20
25
30
°2θ Co Kα

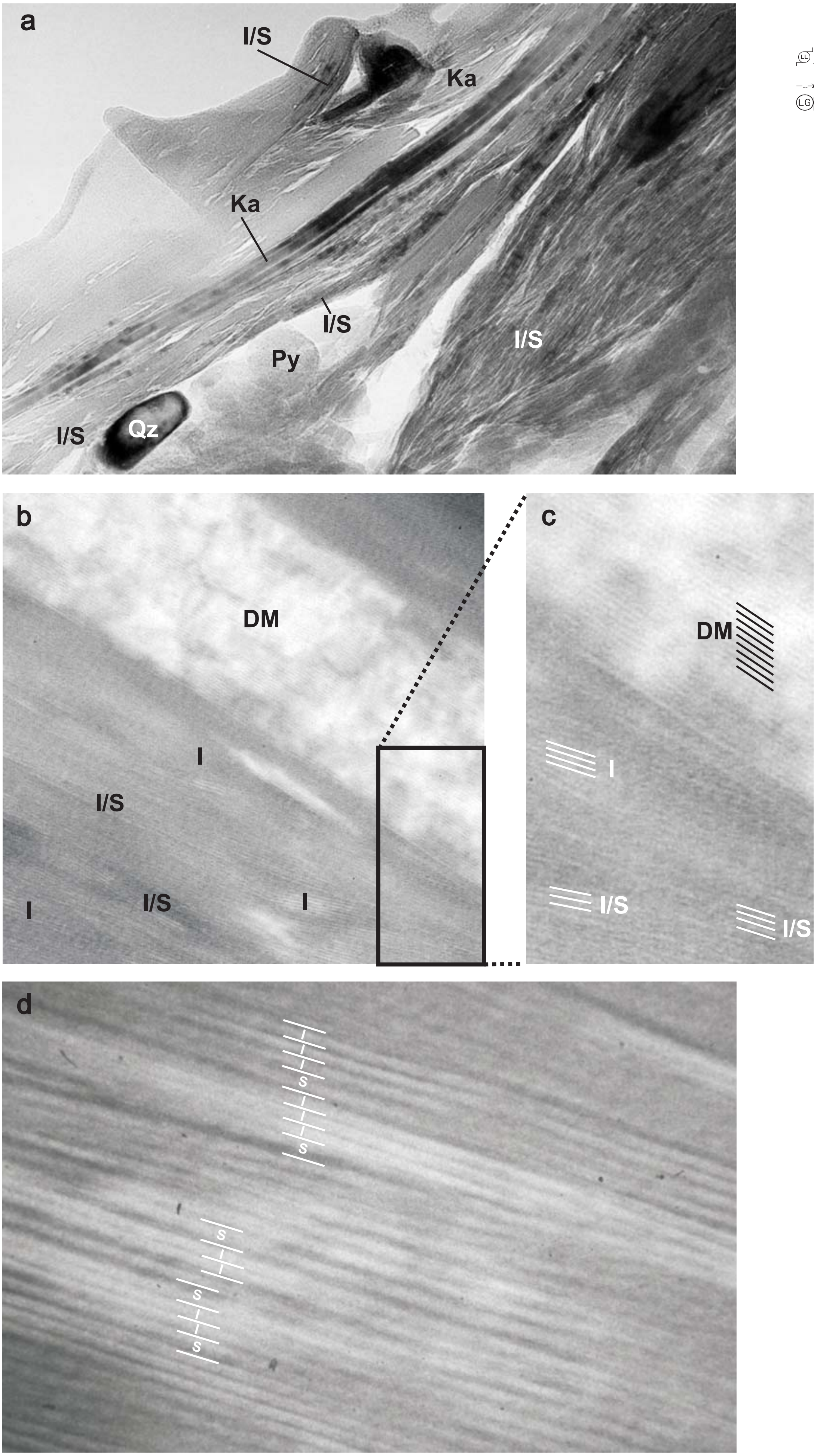
a
I/S
Ka
Ka
I/S
Py
I/S
I/S
Qz
b
DM
I
I/S
I
I/S
I
c
DM
I
I/S
I/S
d
S
S
S
S
S

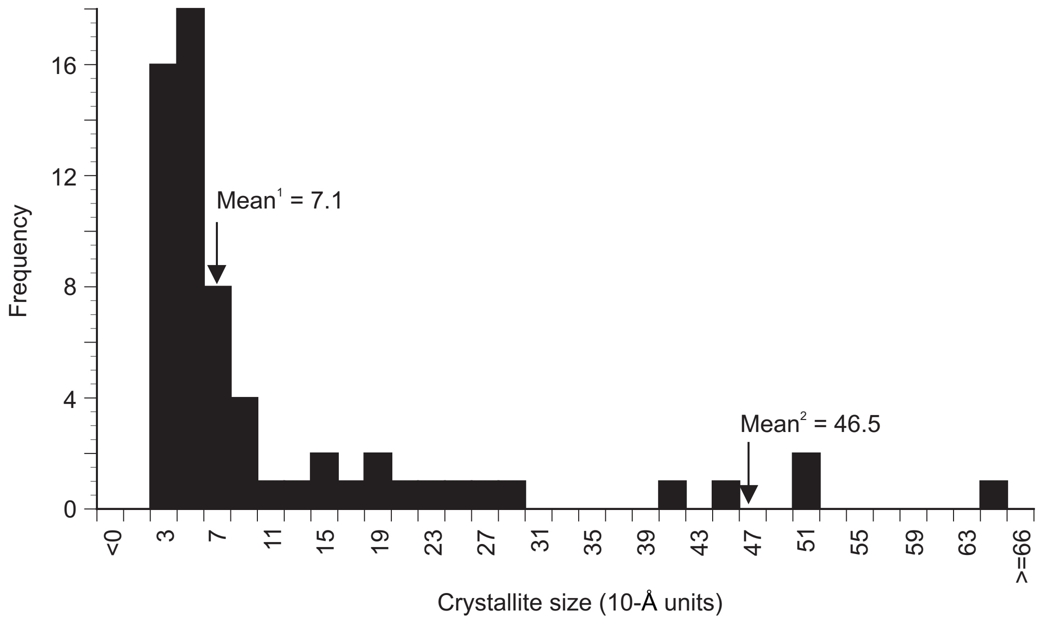

Frequency
0
4
8
12
16
Mean1 = 7.1
Mean2 = 46.5
<0
3
7
11
15
19
23
27
31
35
39
43
47
51
55
59
63
>=66
Crystallite size (10-Å units)

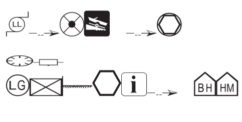

LG
i
BH
HM

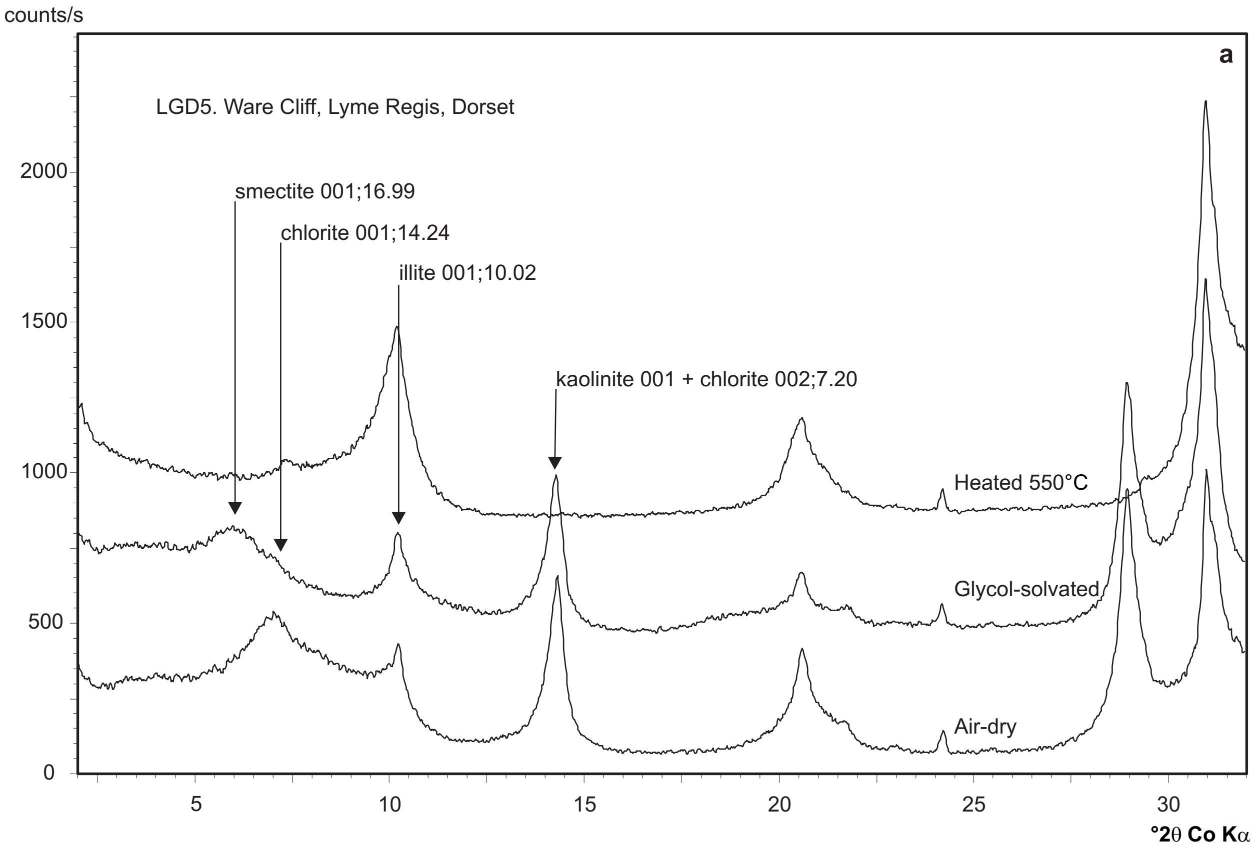

counts/s
a
LGD5. Ware Cliff, Lyme Regis, Dorset
2000
1500
1000
500
0
smectite 001;16.99
chlorite 001;14.24
illite 001;10.02
kaolinite 001 + chlorite 002;7.20
Heated 550°C
Glycol-solvated
Air-dry
5
10
15
20
25
30
°2θ Co Kα

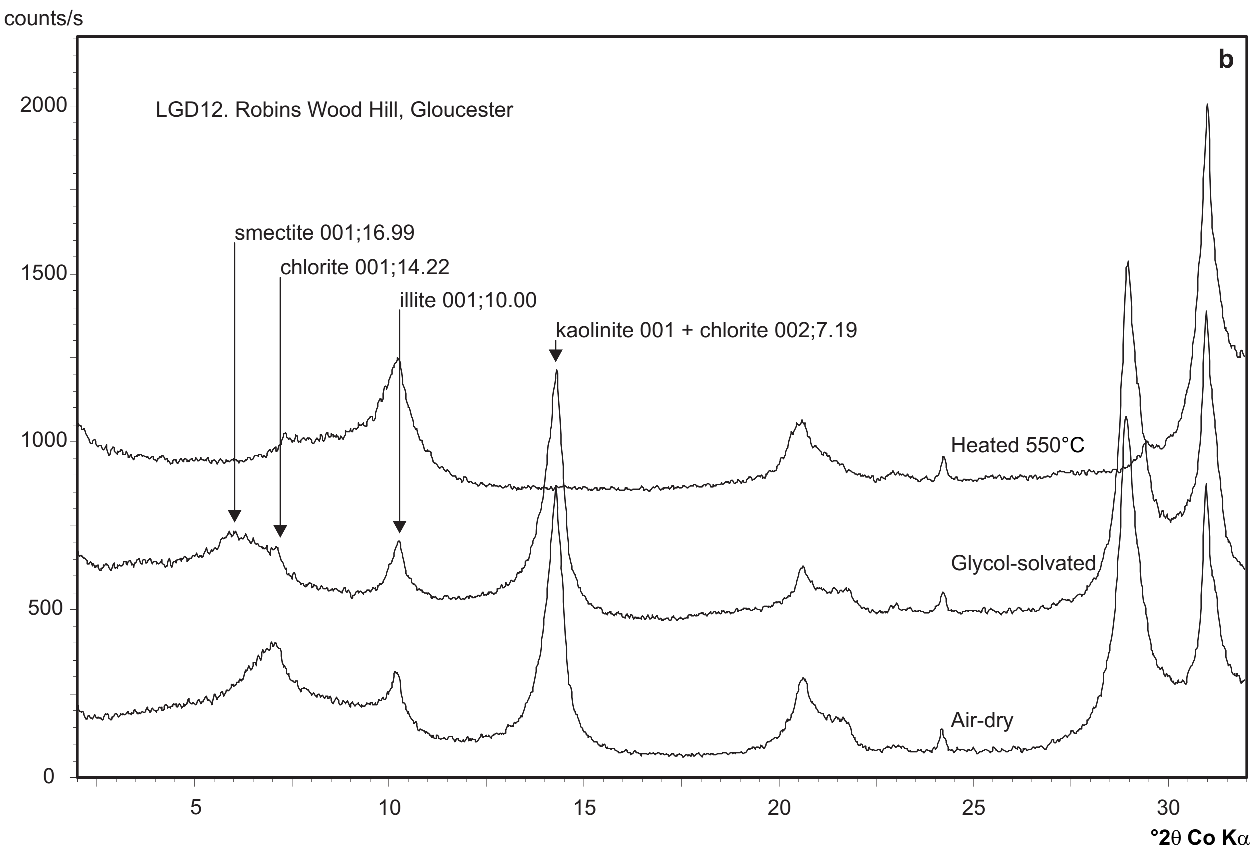

counts/s
b
LGD12. Robins Wood Hill, Gloucester
2000
1500
1000
500
0
smectite 001;16.99
chlorite 001;14.22
illite 001;10.00
kaolinite 001 + chlorite 002;7.19
Heated 550°C
Glycol-solvated
Air-dry
5
10
15
20
25
30
°2θ Co Kα

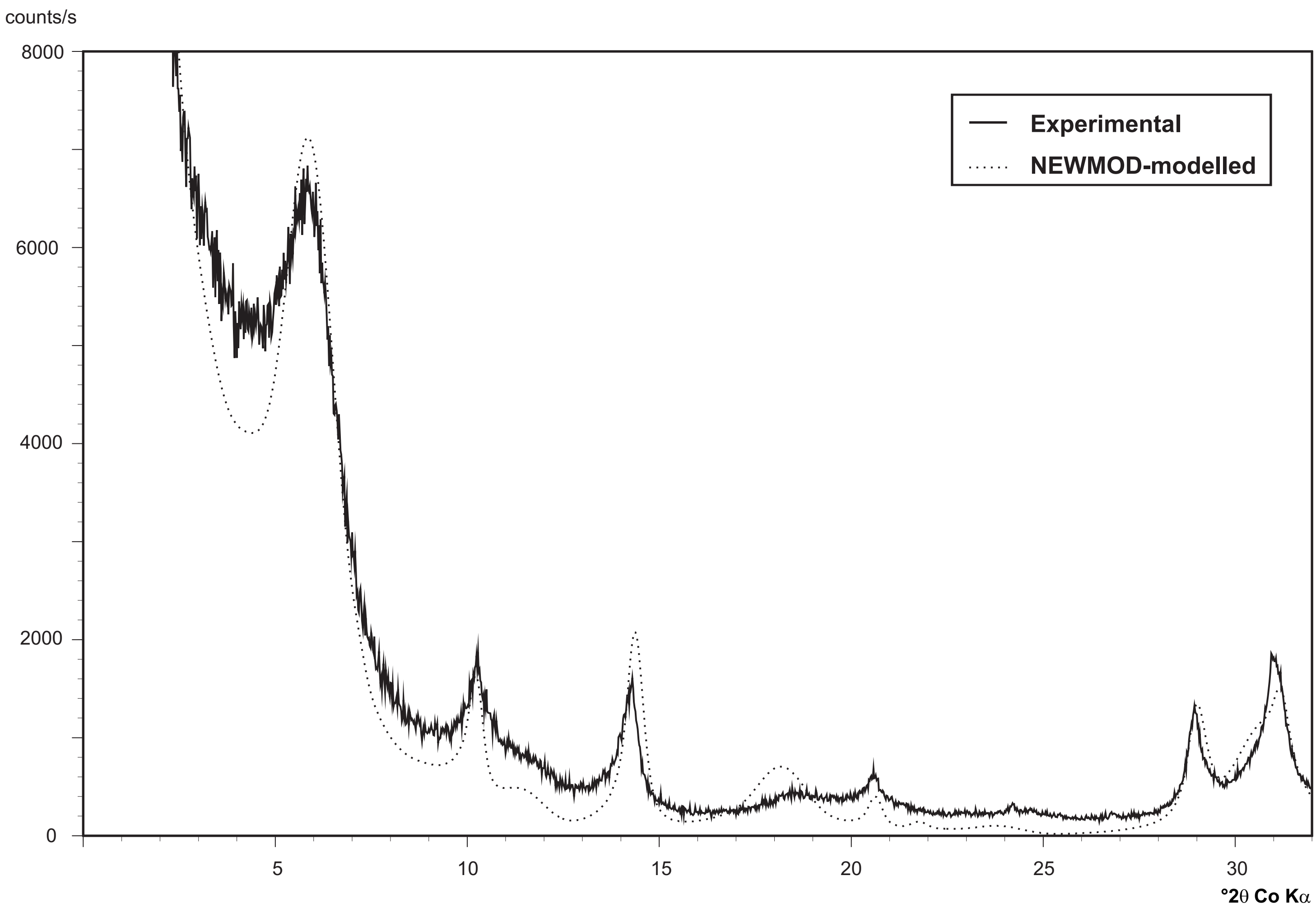
counts/s
8000
6000
4000
2000
0
5
10
15
20
25
30
°2θ Co Kα
Experimental
NEWMOD-modelled